EXPERIMENTAL INVESTIGATIONS OF THE HYDROFORMING PROCESSES PERFORMED ON SEAMLESS TUBE OF AA 7003

Carlo Mapelli[1], Riccardo Riva[1], Roberto Venturini[1], Stefano Locatelli[2]

[1] Dipartimento di Meccanica, Politecnico di Milano, Milano
[2] Dedacciai, Via Leonardo da Vinci 19, Campagnola Cremasca (CR)

Abstract

The hydroforming process is a promising technique for the production of components in complex shapes which may increase stiffness and momentum of inertia. This study has been focused on a complete experimental characterization of hydroformed aluminium seamless tubes. The Al seamless tubes have been marked with circle grids produced by a specifically developed chemical etching based on $CuCl_2$ reactant. During forming, the circle patterns are deformed with the Al alloys and so they permit to measure the local deformation. Moreover, under the hypothesis of volume conservation during plastic deformation, the measurements of the deformed markers allow the evaluation of the thickness variations also as a function of the imposed curvature radius. Finally, the texture analysis has been performed by SEM-EBSD and the development of particular crystallographic textures, which revealed possible residual formability, have been identified. The results represent a preliminary step for further implementation of a simulation activity which will take into account also the forming behaviour of the materials under friction forces produced on the tube during expansion in the die.

Riassunto

Il processo di idroformatura è una tecnologia promettente in grado di realizzare geometrie complesse, allo scopo di incrementare rigidità e momento di inerzia di alcuni componenti. Questo studio consiste nella caratterizzazione sperimentale dello stato di deformazione di tubi senza saldatura in alluminio idroformati. Sui tubi è stata ricavata una opportuna marcatura, attraverso un attacco chimico a base di $CuCl_2$. Durante il processo, la marcatura subisce la stessa deformazione del tubo, permettendo così di verificare localmente lo stato di deformazione. Inoltre, sfruttando l'ipotesi di costanza del volume durante la deformazione plastica, la misura dei marcatori deformati ha permesso di valutare la variazione dello spessore, in funzione del raggio di curvatura imposto. Infine, è stata analizzata la tessitura cristallografica con la tecnica SEM-EBSD, portando alla individuazione delle componenti di tessitura sviluppate.
Lo scopo di questo tipo di attività è quello di fornire un supporto alla simulazione dei processi, tenendo in considerazione anche il comportamento del materiale sottoposto alle forze di attrito sviluppate durante l'espansione nella cavità dello stampo, attraverso il contatto con le pareti.

INTRODUCTION

Tube hydroforming (THF) is a metal forming process through which the tubes are formed into complex shapes within a die cavity by the simultaneous application of internal pressure and axial compressive forces (Figure 1) [1,2,3].
An increasing acceptance and application of this technology demands a full understanding of interaction among the processing variables for a sound, and defect-free component. An overall review of the hydroforming process can be found in several publications [1-8] when the general conclusion that for steel tube the maximum strain which can be imposed is in the range of 0.1 - 0.7. has been reached.
In hydroforming of the tubes the ultimate goal is to form a blank tube of uniform cross-section into complex shape with varying cross-sections without causing forming instability like bursting, necking, wrinkling or buckling. The overall success of hydroforming heavily depends on the incoming tubular material properties [1,8,9,10,11,12]: yield and tensile strength, ductility and anisotropy. The effect of the strain-hardening exponent (*n*-value) and of the plastic anisotropy (*r*-value) depends on the crystallographic orientation and can affect the developed internal pressure, the wall thickness distribution and the maximum expansion [13]. The control of tube production and of the annealing process needs to be carefully managed to produce a tube with desired properties.
In the work an experimental evaluation of strains in complex shape sections of hydroformed tubes was conducted by studying the influence of two different internal pressures on the crystallographic textures affecting the formability performances of the materials.
The aim of this study is the experimental determination of the local strain of the thinning realized on seamless tube of AA7003 as a function of the imposed curvature radius and of the friction developed by the contact between the tube and the die wall. The determination of the textures performed by SEM-EBSD analysis on the hydroformed aluminium tube has allowed to associate the texture evolution with the strain imposed by the hydroforming system and by the applied operating parameters.
This step can represent a fundamental issue for the implementation and validation of a reliable computational model taking into account the macroscopic stress strain relations, the interaction among the tube and the die walls and the evolution of the involved crystallographic textures.

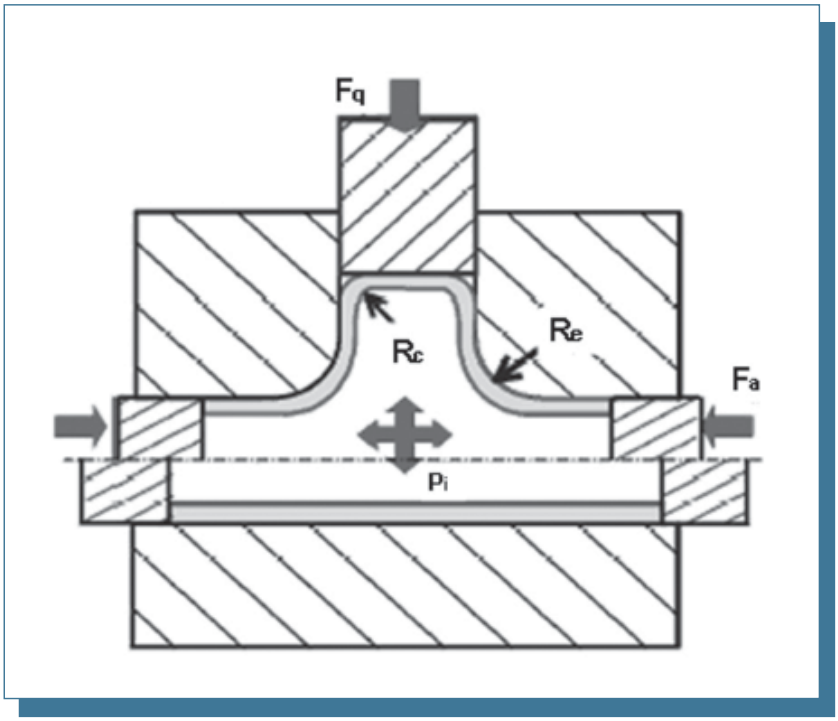

Fig. 1: Elements of a typical THF process. (F_a) Axial Force, (F_q) counter Force, (P_i) internal pressure, (R_c) corner radius, (R_e) fillet radius [1].

EXPERIMENTAL PROCEDURE

The hydroforming experiments have been performed on AA7003 seamless tubes whose chemical composition [14] and the related mechanical properties are reported in tables 1 and 2, respectively. Before the hydroforming operation the wiredrawn tube underwent an annealing treatment at 390 °C for 2h and a successive controlled cooling in furnace to a temperature of 250 °C and then the tube has been cooled in quiet air to room temperature. The hydroforming of the tube has been performed 35h after the end of the annealing treatment.

TABLE 1 - MEASURED CHEMICAL COMPOSITION OF AA7003 (WT%)

%wt	Si	Fe	Cu	Mn	Mg	Cr	Zn	Ti	Pb	Zr	Bi	Sn	Ni
Contents	0.153	0.257	0.031	0.176	0.838	0.120	5.505	0.029	0.003	0.1505	0.0001	0.0020	0.0040

Table 2 - Mechanical properties before the hydroforming operation

Mechanical properties	R_m [N/mm²]	$R_{p0.2}$ [N/mm²]	A_5 [%]	A_{20} [%]	HB
	186	94	21	17.5	52.4

The textures of the tube have been measured before and after the hydroforming procedure through the SEM-EBSD technique, and the polar diagram, the inverse polar diagram and the ODF (Orientation Distribution Fucntion) have been determined.

The tube surface have been drawn by a chemical etching producing a round shape grid. The grid should resist to the high friction produced by the contact between the tube and the die allowing a correct measurement of the resulting grid circles.The round shape of the markers was chosen because it allowed a rapid evaluation of the strain along different directions. The circles of the grid were 4 mm diameter and the distance between the centres of two adjacent circles was 6 mm.

The tube external surface was pickled through a solution of NaOH (30 g/dm³), at 35 ÷ 40 °C for 180 ÷ 300 s and then was dipped into a solution 33% HNO_3, at room temperature for 30 ÷ 45 s and dried. The tube was covered by adhesive polyethilene film with a sequence of circles representing the grid dipped in a solution of $CuCl_2 \cdot 2H_2O$ (10 g/dm³), H_2SO_4 (90 g/dm³), at room temperature for 105 ÷135s and finally washed by immersion in tap water for 300s and dried by forced air at 45°C (Figure 2). Each circular array of round shape markers (at a certain distance from the tube end) is composed of 22 elements. The circle grid analysis have been operated along four different directions: 0°, 45°, 90°, 135° rotated directions from the tube axis (Figure 3, Figure 4).

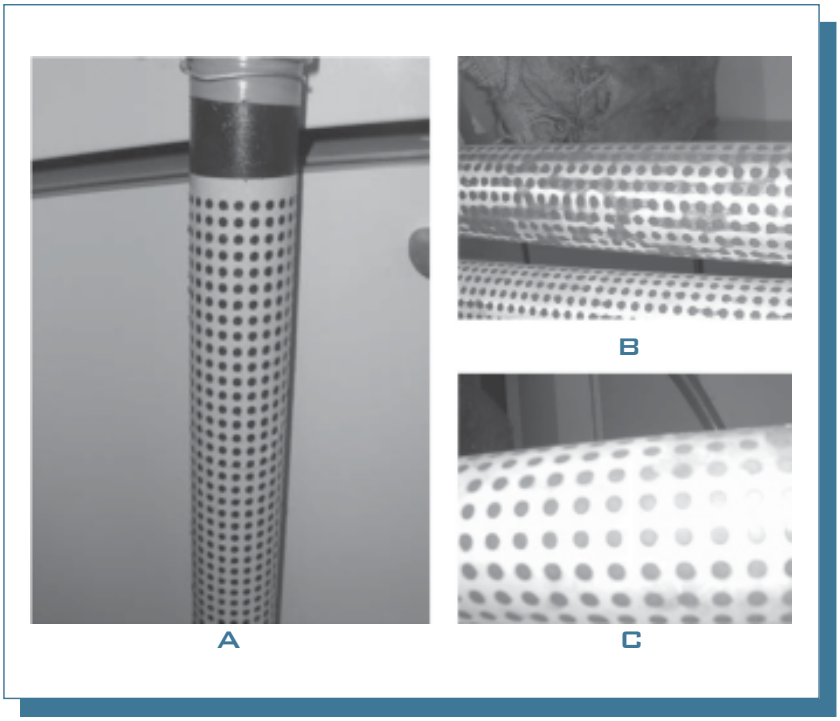

Fig. 2: An example of the grid produced on the tube before the hydroforming procedure after the extraction from the etching bath (a), after drying (b) and scrubbing (c).

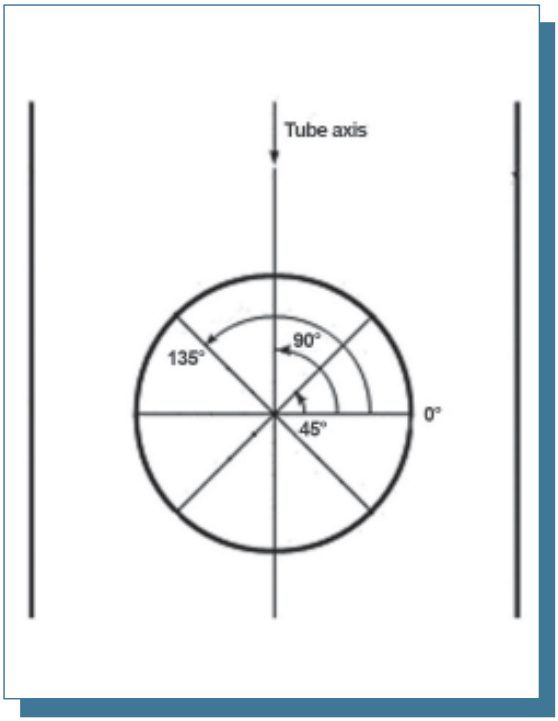

Fig. 3: An example of the grid produced on the tube before the hydroforming procedure after the extraction from the etching bath (a), after drying (b) and scrubbing (c).

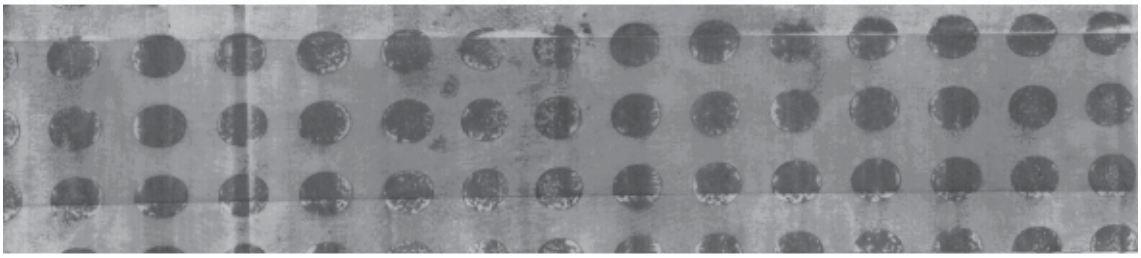

Fig. 4: Adhesive layer showing the traces of the deformed round shape markers.

The shape of the deformed markers, can be easily revealed through an image analyser which permits the successive computation of strain by the well known formula:

$$\varepsilon_x = \ln \frac{d}{d_0} \qquad (1)$$

A precise determination of the local deformation produced on the tube wall under the hypothesis of the volume conservation during the plastic deformation allows the computation of the local thinning.

The SEM-EBSD analysis has been performed with the following operative parameters: magnification 150X, pixel resolution 20 °m^2, accelerating voltage 20 kV.

In each analysis an area of 2 mm^2 has been investigated to grant the statistical reliability of the crystallographic data. The reference system has been set so that the RD direction has been set parallel to the tube one and the ND is always perpendicular to the external profile of the investigated tube section. The textures have been identified before and after the hydroforming.

The hydroforming experiments have been performed on a tube: 780 mm long, 1.5mm thick and with an external diameter of 46 mm. The length of the tube extremities forbidden to expansion was 55 mm.

After lubricant deposition the experiments have been realized at two different levels of the maximum internal pressure: 36 MPa and 81 MPa. The deformation pattern of the formed tube has been analysed in correspondence of four section taken at 188, 442, 592, 706 mm from the reference extremity (Figure 5).

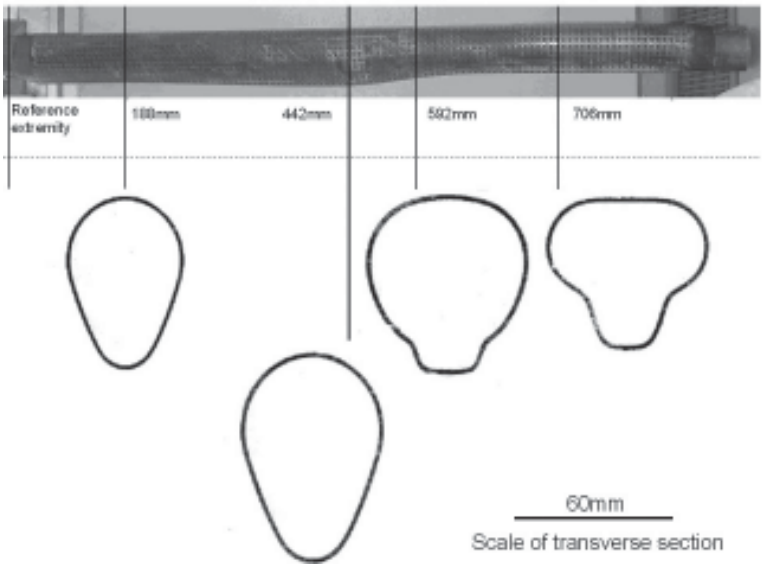

Fig. 5: The position of the investigated transverse sections. The represented transverse sections are the real ones digitally scanned to represent the real shape after the cutting and the size scale has been indicated to allow the correct interpretation of the represented figures.

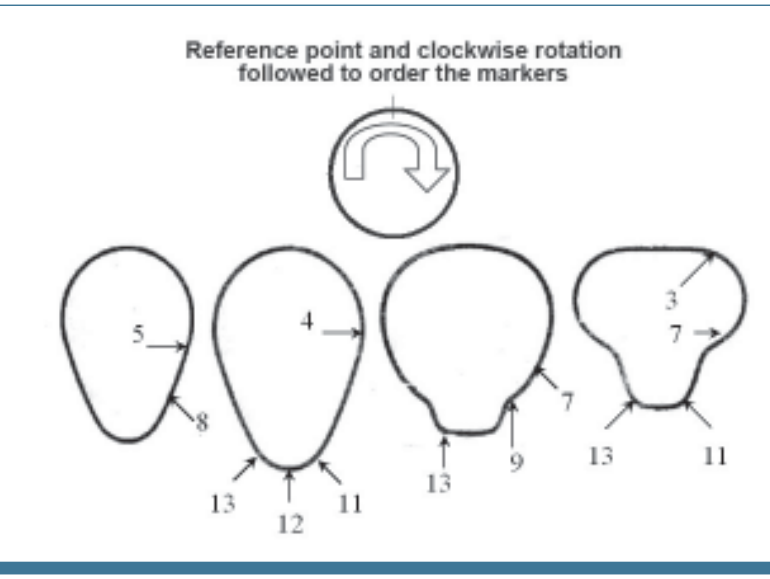

Fig. 6: Identification of some significant numbered markers on the analysed transverse section.

Fig. 7: Circle grid analysis in correspondence of the two applied levels of internal pressure.

RESULTS

The results related to the revealed state of deformation have been associated to each measured strained marker and its identification has been performed through a correct numbering of the 22 round shape markers corresponding to a specific section. The markers composing the array belonging to a particular section have been ordered through a clockwise rotation from the upper point of the section taken as the reference position (Figure 6). The maximum strains belong to the sections located at 442 mm, 592 mm and at 706 mm featured by the smallest imposed curvature radius

and by the possible change of the profile concavity (Figure 7, Figure 8). The principal deformations featuring a material can be identified through the determination of at least three strains interesting three different directions on a plane [15].

The high deformations reached in the section at 442 mm from the extremity can be expected without particular surprise, because this is the section in which the down part of the hydroformed tube underwent the largest expansions and the largest displacement in correspondence of the markers 10 and 11, but it is interesting that the highest applied internal pressures

Fig. 8: Principal deformations computed on the basis of the sizes of the circle grid analysis of the two applied levels of internal pressure.

seem to increase the homogeneity of the deformation induced in the tube wall.

On the other hand, the presence of changes of concavity and the imposition of small curvature radius, as the ones realized in the sections 592 mm and 706 mm from the reference extremity, implies some incoming critical situations in the deformation states as well.

The evolution of the textures from the crystallographic situation before the hydroforming is clear (Table 3).

The revealed textures are consistent with the revealed deformation state. In particular, a sharp increase of the texture components featured by planes {001} tangent the contour profile of the wall (i.e. $\{010\}<001> - \{010\}<101> - \{001\}<\bar{1}\bar{2}0>$) characterizes the regions interested by the largest deformations. These texture components have been revealed in correspondence of the points which underwent the most significant deformations and, using a logarithmic scale, their statistical intensities, if compared with a random distribution, assume the value of 8 which is characteristic of very sharp texture components. This phenomenon is related to a progressive decreasing of the favourable texture components characterized by {011} and {111} planes and an intensification of the ones featured by {123} and {001} (Table 4).

Table 3 - Texture components revealed in the AA7003 before the hydroforming

Textures components	Intensity (log scale)
$\{110\}<001>$ $\{110\}<111>$ $\{114\}<132>$	(8)(8)(8)(7)

Table 4 - Texture components revealed in the AA7003 at different deformation condition.

Applied internal pressure	Region		Region		Region	
	Under marker 3 of each section	Intensity (log scale)	Under marker 13 of the section at 442, 592, 706mm	Intensity (log scale)	Under marker 12 of the section at 592, 706mm	Intensity (log scale)
36MPa	Isotropy γ-fiber {010}<001>	(5) (5-6)	$\{010\}<001>$ $\{124\}<2\bar{3}1>$ $\{010\}<101>$ $\{001\}<1\bar{2}0>$ γ-fiber $\{11\}<1\bar{2}1>$ *to* $\{11\}<1\bar{2}1>$	(8) (8) (7) (7) (6-7)	$\{012\}<100>$ $\{124\}<2\bar{1}0>$ $\{124\}<23\bar{1}>$ $\{001\}<100>$ $\{011\}<3\bar{2}\bar{2}>$ $\{011\}<1\bar{1}1>$ $\{011\}<1\bar{1}2>$ $\{11\}<1\bar{2}1>$	(8) (8) (8) (8) (7-8) (7) (7) (7)
81MPa	Isotropy γ-fiber {010}<001>	(4-5) (6)	$\{011\}<0\bar{1}1>$ $\{001\}<\bar{1}\bar{2}0>$ $\{001\}<\bar{1}30>$ $\{14\}<2\bar{6}1>$ γ-fiber $\{11\}<1\bar{2}1>$ *to* $\{11\}<0\bar{1}1>$ $\{332\}<1\bar{2}1>$ $\{124\}<2\bar{1}0>$	(8) (8) (8) (8) (7-8) (7) (7)	$\{125\}<1\bar{2}1>$ $\{123\}<2\bar{2}1>$ $\{001\}<\bar{1}30>$ $\{001\}<0\bar{1}0>$ α-fiber $\{011\}<001>$ γ–fiber $\{11\}<1\bar{2}1>$ *to* $\{11\}<0\bar{1}1>$	(8) (8) (8) (7-8) (7-8) (7) (7) (7)

DISCUSSION

A good fitting has been found among the deformations measured through the thickness and the ones computed under the hypothesis of volume conservation on the basis of the values of the deformation revealed along the direction parallel and perpendicular to the tube axis. So, the measured deformations along the direction perpendicular and parallel to the tube axis ($e_{0°}$;$e_{90°}$) can be assimilated to the principal deformations (e_{I},e_{II}). This result implies that the principal deformation directions correspond to the direction parallel and perpendicular to the tube axis, although after a first approximate sight the overall deformation patterns can appear as very complex in order to realize such a complex shape. Thus, the deformation through the thickness can be considered the third principal component of deformation (e_{III}).

The increase of the internal pressure can permit the decreasing of the localized wall thinning. This is extremely advantageous because such a situation grant a lower thinning of the tube wall avoiding the plastic instability which can take place in the presence of an excessive reduction of the tube thickness. The evaluation of the experimental results clearly indicates that the application of the highest internal pressure can favour a more homogeneous plastic behaviour. This situation should be confirmed also by a successive dynamic structural simulation, but it seems to be due to the fact that, in presence of a low internal pressure, the points characterized by a change of concavity or by a restriction of the section profile can constitute an obstacle to the plastic flow of the material which enters in contact with the forming die. So, those points represent the constraint points for the material to be formed, due to the frictions developed by the relative motions among the die walls and the material during its deformation. The imposition of the highest pressure levels can certainly produce an increase of the friction forces, but can also contribute to increase the plastic flow of the material on those critical points, favouring the thinning and the general plastic flow of the material towards the other regions of the material, which have not already reached the final point of their displacement on the die surface. In presence of the highest pressure levels in the constraints points the tube wall is subject to a greater thinning, but this reduces the thinning experienced by the other material regions which are still under deformation to reach the die surface. Thus, the application of the highest internal pressure makes the wall thickness more homogeneous and decrease the possibilities to meet the conditions of the plastic instability.

The induced textures point out a satisfactory consistency with the defined measured deformation states and, provided a specific point, they do not present significant variations between the inner and the outer region of the wall thickness. Actually, the regions featured by the largest deformations show the texture components with the lowest formability and there is a well defined pattern of crystallographic organization which leads from the isotropy to the well formable textures featured by the {111} and {011} planes perpendicular to the normal of the profile section and from the weakening of these last ones to a progressive increasing of the textures featured by {001} and by the textures near the β-fiber (i.e. {123}-{124}) which is associated to the decrease of the intensity of the textures belonging to the α-fiber and γ-fiber. On the other hand, the application of the highest internal pressure allows to realize also a more homogeneous distribution of the crystallographic orientation and to slower the reaching of {001}<001> (Cube texture) preserving the formability and the thoughness of the material [16].

CONCLUSION

This preliminary study about the experimental evaluation of the local deformations and about the development of the crystallographic textures induced within the hydroformed tube allows to state that:

- the procedure based on the chemical etching and designed to produce a grid suitable for the experimental identification of the local deformation hydroformed tube has been tested and it can be considered as extremely reliable;
- the most critical sections are those interested by a significant thinning and by the largest expansions, by the smallest imposed curvature radius and by a possible change of the profile concavity;
- the increase of the imposed internal pressure allows the tube to obtain a more homogeneous state of deformation and of crystallographic textures. The highest internal pressure can be balanced by the constraint effects produced on the tube displacement by the change of concavity or by the restriction of the profile section. The larger thinning takes place in the points of the section constrained by the highest friction and this phenomenon seems to improve the plastic flow of the materials in these regions, so that they can provide a larger quantity of material to the regions which have not already reached the die surface;
- the strongly deformed regions are featured by the decreasing of {111} and {011} planes perpendicular to the normal section with a simultaneous increasing of the textures featured by {001} and by the textures near the β-fiber, (i.e. {123}-{124}) and the decreasing of the intensity of the textures belonging to the α-fiber and γ-fiber: this degeneration of the crystallographic texture points out a reduction of the formability and toughness resources associated to the hydroformed alloy.

REFERENCES

[1] M. Koç, T. Altan, An overall review of the tube hydroforming (THF) technology, *J. Materials Processing Technology*, 108 (2001), pp. 384 – 393.

[2] M. Koç, T. Altan, Prediction of forming limits and parameters in the tube hydroforming process, *J. Materials Processing Technology*, 42 (2002), pp. 123 – 138.

[3] F. Dohmann, Ch. Hartl, Tube hydroforming—research and practical application, *J. Materials Processing Technology* , 71 (1997), pp. 174 – 186.

[4] E. Chu, Yu Xu, Hydroforming of aluminum extrusion tubes for automotive applications. Part I: buckling, wrinkling and bursting analyses of aluminum tubes, *International Journal of Mechanical Sciences*, 46 (2004), pp.263-283.

[5] E. Chu, Y. Xu, Hydroforming of aluminum extrusion tubes for automotive applications. Part II: process window diagram, *International Journal of Mechanical Sciences*, 46 (2004), pp.285-297.

[6] K. Manabe, H.Nishimura, J. Eng. Mater. Technol., 100 (1978), pp. 421-425.

[7] S. Fuchizawa, Advanced Technology Plasticity, 1 (1984), pp. 297-302.

[8] S. Fuchizawa, Advanced Technology Plasticity, 2 (1987), pp. 727-732.

[9] L.H. Lang, Z.R. Wang, D.C. Kang, S.J. Yuan, S.H. Zhang, J. Danckert, K.B. Nielsen, Hydroforming highlights: sheet hydroforming and tube hydroforming, *Journal of Materials Processing Technology*, 151 (2004), pp. 165 – 177.

[10] S.H. Zhang, Developments in hydroforming, *J. of Materials Processing Technology*, 91 (1999), pp. 236 – 244.

[11] H. Y. Li, X.S. Wang, S.J. Yuan, Q.B. Miao, Z.R. Wang, Typical stress states of tube hydroforming and their distribution on the yield ellipse, *Journal of Materials Processing Technology*, 151 (2004), pp. 345 – 349.

[12] N. Asnafi, Analytical modelling of tube hydroforming, *Thin – Walled Structures*, 34 (1999), pp. 295 – 330.

[13] U. Lucke, Ch. Hartl, T. Abbey, Hydroforming, *Journal of Materials Processing Technology*, 115 (2001), pp. 87 – 91.

[14] UNI-EN 10204.

[15] L. Corradi Dell'Acqua, Meccanica delle Strutture, McGraw Hill, Milano (1992), pp.116-120.

[16] M. Hatherly, W.B. Hutchinson, An Introduction to Textures in Metals (Monograph No. 5). London, The Institute of Metals, 1979, 45-57.

LIST OF SYMBOLS

e_X deformation measured along the generic direction *X*.

d_X measured final diameter of the round shape marker along the generic direction X.

d_0 initial diameter of the round shape marker.